Algorithm Theoretical Basis Document for MSG/SEVIRI Sea Surface Temperature data record

OSI-250

DOI:10.15770/EUM_SAF_OSI_0004

Version: 1.3
Date: 26/1/2018

S. Saux Picart

Documentation change record

Version	Date	Authors	Description
1.0	15/3/2016	MF/CMS	Initial submitted version
1.1	31/5/2016	MF/CMS	Updated version taking into account RIDs from PCR. In particular: • Clarification of the main steps of the processing with addition of references to following sections in section 2.1. • Addition of details about the test indicators in section 2.3. • Explanation about why we retrieve sub-skin SST in section 4.
1.2	15/12/2017	MF/CMS	Updated version for the DRR with clarifications where methodologies were not described precisely in version 1.1. This includes: • Addition of the SST algorithm coefficient for MSG-2 • Clarification about the twilight retrieval of SST section 4 • Addition of details about the brightness temperature adjustment and algorithm correction sections 4.2 and 4.1 • Clarification on SSES 6 • Addition of details about hourly synthesis 5
1.3	26/1/2018	MF/CMS	More precise reference to SVR for SSES in section 6.

Contents

List of Figures

List of Tables

1 Introduction

The EUMETSAT Satellite Application Facilities (SAFs) are dedicated centres of excellence for processing satellite data. They form an integral part of the distributed EUMETSAT Application Ground Segment. The Ocean and Sea Ice SAF, led by Météo-France/Centre de Météorologie Spatiale (MF/CMS), has the responsibility of developing, validating and distributing near real time products of Sea Surface Temperature (SST), radiative fluxes, wind and Sea Ice for a variety of platforms/sensors.

As part of the Second Continuous Development and Operations Phase (CDOP-2) OSI SAF (more specifically MF/CMS) has committed to reprocess Sea Surface Temperature from MSG/SEVIRI archive from 2004 to 2012.

1.1 Purpose and scope of the document

This document describes the algorithms and methods implemented for MSG/SEVIRI SST data record, it also gives an overview of the processor and of the datasets used. This reprocessing activity aims at providing users with the dataset labelled OSI-250 which characteristics are summarised here (extracted from the Product Requirement Document [AD.1]):

Table 1: Extracted from [AD.1]. Threshold, target and optimal accuracies define respectively: the lower limit of usefulness, the main reference for assessment at EUMETSAT and the optimal performance reachable in theory provided the instrument characteristics

Product ID	Spatial coverage	Spatial sampling	Threshold accuracy. Monthly bias, STD	Target accuracy. Monthly bias, STD	Optimal accuracy. Monthly bias, STD
OSI-250	60°N to 60°S and 60°W – 60°E	0.05°	1°C, 1°C	0.3°C, 0.8°C	0.1°C, 0.3°C

This document is complemented by the MSG/SEVIRI Sea Surface Temperature data record Scientific Validation Report [RD.2] and MSG/SEVIRI Sea Surface Temperature data record Product User Manual [RD.3].

1.2 Scientific motivations

SST retrieval from infra-red (IR) radiometer measurements classically uses multichannel algorithms (e.g. McCain et al., 1985). More recent developments have improved retrieval through the usage of atmospheric profiles of temperature and water vapour provided by Numerical Weather Prediction models in order to correct for regional and seasonal biases. Merchant et al. (2008) have developed the Optimal Estimation method and Le Borgne et al. (2011) have developed an algorithm correction approach. In the past few years, OSI SAF has been using the algorithm correction method in the development of the newer processing chains. The reprocessing of MSG/SEVIRI archive is an opportunity to develop a framework to test both methods rigorously on a large spatial and temporal scales. This work will then provide a benchmark for the future developments of SAF OSI processing chains.

From a user's prospective, the reprocessing of MSG/SEVIRI SST will provide a unique dataset for many scientific applications. Its temporal and spatial resolution will provide valuable information for studying diurnal variability of SST, ocean surface dynamics, ocean-atmosphere energy and gas exchange... Its homogeneity will further interests groups involved in data assimilation and reanalysis production. The data record provided by the OSI SAF reprocessing is complementary to the work done under the ESA SST Climate Change Initiative which aim is to provide a consistent SST reprocessing from infra red measurements aboard low earth orbiting satellite.

1.3 Reference documents

Ref	Title	Code
[RD.1]	Data Set Generation Capability Description Document for MSG SST reprocessing (OSI-250)	SAF/OSI/CDOP2/MF/TEC/TN/231
[RD.2]	MSG/SEVIRI Sea Surface Temperature data record Scientific Validation Report - OSI 250	SAF/OSI/CDOP3/MF/SCI/RP/310
[RD.3]	MSG/SEVIRI Sea Surface Temperature data record Product User Manual - OSI 250	SAF/OSI/CDOP3/MF/TEC/MA/309
[RD.4]	MSG Level 1.5 Image Data Format Description	EUM/MSG/ICD/105 v7
[RD.5]	Product User Manual SEVIRI cloud mask data set CM-21012	SAF/CM/DWD/PUM/SEV/CLM v1.1

1.4 Applicable documents

Ref	Title	Code
[AD.1]	Ocean and Sea Ice SAF CDOP-2. Product Requirement Document version 3.3	SAF/OSI/CDOP2/MF/MGT/PL/2-001

1.5 Acronyms

AOD	Aerosol Optical Depth
AVHRR	Advanced Very High Resolution Radiometer
BT	Brightness Temperature
CMC	Canadian Meteorological Centre
ECMWF	European Centre for Medium-range Weather Forecasts
ESA	European Space Agency
GDS	GHRSST Data Specification
GHRSST	Group for High Resolution SST
GTS	Global Telecommunication System
IR	Infra-Red
LEO	Low Earth Orbiter
MF/CMS	Météo France/Centre de Météorologie Spatiale
MDS	Matchup DataSet
Metop	Meteorological Operational
NAR	North Atlantic Region
NOAA	National Oceanic and Atmospheric Administration
NWP SAF	Numerical Weather Prediction Satellite Application Facility
OSI SAF	Ocean and Sea Ice Satellite Application Facility
OSTIA	Operational Sea Surface Temperature and Sea Ice Analysis
QL	Quality Level
RTM	Radiative Transfer Model

RTTOV	Radiative Transfer for TOVS
SAF	Satellite Application Facility
SDI	Saharan Dust Index
SEVIRI	Spinning Enhanced Visible and InfraRed Imager
SSES	Sensor Specific Error Statistics
SST	Sea Surface Temperature
STD	Standard Deviation
SZA	Solar Zenith Angle
TIROS	Television Infrared Observation Satellite
TOVS	TIROS Operational Vertical Sounder

2 Overview of the reprocessing

In this section a brief overview of the input datasets used and the main steps of the reprocessing are given.

2.1 The main steps of the reprocessing

The reprocessing is divided into steps, each step being applied to the whole dataset:

1. *Simulations of Brightness Temperature (BT)*: The Radiative Transfer for TOVS (RTTOV, Saunders et al. (1999)) model version 11 simulated BTs are computed for every clear sky sea and lake pixels and for each IR channel used for SST retrieval and every three hours. See section 4.2 for details.

2. *Saharan Dust Index (SDI)*: It is used for downgrading the quality level of pixels contaminated by atmospheric dust aerosols (see section 2.3) and eventually correcting retrieved SST (see section 4.4). The computation of SDI is based on the principle of Merchant et al. (2006) during night-time and interpolated during daytime (see section 3).

3. *Control of the mask*: This step is designed to detect possible problems such as remaining cloud contamination. It consists on a series of tests which are contributing to the Quality Level (QL) assignment (see section 2.3). These tests are performed at various stage of the reprocessing depending on the tested values.

4. *SST retrieval*: A classical non-linear SST algorithm is used to provide a first estimate of the SST (see section 4.1). It is used in particular in the control of the mask. An algorithm correction (section 4.3) is used to correct for regional and seasonal biases with respect to drifting buoys measurements.

5. *Single Sensor Error Statistics (SSES)*: bias and standard deviation of the error relative to drifting buoy measurements are added (see section 6).

2.2 Data

The list of reference datasets used in the confection of the MSG/SEVIRI SST data record is:

- 3-hourly atmospheric temperature and humidity profiles (plus a few surface fields) from ERA-Interim on 37 pressure levels on a global $0.5° \times 0.5°$ grid from ECMWF (Dee and 35 co-authors, 2011).

- OSTIA daily SST re-analyses (2004-2007) (Roberts-Jones et al., 2012) and analyses (2008-2012) (Donlon et al., 2012) on a global $0.05° \times 0.05°$ grid from UK Met Office.

- SST climatology derived from OSTIA daily SST re-analyses (1985-2007) (Roberts-Jones et al., 2012).

- MSG-1 and MSG-2 visible and infra-red SEVIRI level 1.5 reprocessed (from January 2004 to 5th of May 2008) and near real-time (from 5th of May 2008 to December 2012) data from EUMETSAT central facility [RD.4].

- Corresponding SEVIRI cloud mask at full space and time resolution, reprocessed by the CM SAF using the NWC SAF MSG V2012 software [RD.5]

- In-situ data set described in Atkinson et al. (2014) created under the SST CCI project.

2.3 Quality level and test indicators

We use the concept of indicator to quantify, in an empirical way, the risk of having an error in the SST retrieval because of uncertainties in algorithms or ancillary variables. For each test, the tested quantity (tested_value) is compared to a limit value (limit_value) and to a critical value (critical_value). Outside this range there is either no problem or the risk of error is too high. The core definition of the test indicator is given below, however many other factors can influence each indicators (for example availability of ancillary data used in the definition of the indicator) that are not detailed here:

$$\text{test\_indicator} = 100(\text{tested\_value} - \text{limit\_value})/(\text{critical\_value} - \text{limit\_value}) \quad (1)$$

There is a range of test_value, for example: the difference between the climatological SST and the retrieved SST, the SDI, the distance to cloud, etc. [limit_value, critical_value] define a range of the test_value below and above which the test_indicator is 0 and 100 respectively.

The formulation above has the advantage of homogenising all the indicators on a unique scale:

- 0: no problem
- $]0, 100[$: potential problem
- 100: critical problem

There are two types of indicators: (i) the common indicators, independent of the SST retrieved and the algorithm used, they are generic to the whole processing. They include the dust indicator, the distance to cloud indicator and the ice indicator. (ii) The specific indicators, based on the value of the SST retrieved in comparison to climatologies of SST and SST gradients (the SST value indicator and the SST gradient indicator). At the end of the processing all these indicators are combined into one single indicator by means of a weighted average: this is the SST mask indicator.

Two other indicators are defined that do not enter in the SST mask indicator, but are considered for determining the quality level: the indicator reflecting the uncertainties of the SST algorithm with respect the satellite zenith angle (algorithm indicator), and the indicator about the confidence we have in the correction term (the SST correction indicator).

A brief description of the tests is given in table 2:

Table 2: List of indicators contributing to the quality level

Test	Description/purpose
SST value	This test aims at attributing a lower quality level to SST values too different from climatology. The local value of estimated SST is compared to a climatology of SST, the larger the difference between estimated SST and SST climatology, the higher the indicator.
SST spatial variability	The main objective of this test is to attribute a lower quality level to pixels in areas where the gradients are unrealistically large due to the presence of undetected cloud cover in most cases. The local value of the SST gradient is compared to a climatology of maximum gradient.
SST temporal variability	The main objective of this test is to attribute a lower quality level to pixels displaying a fast changing SST suggesting that some cloud contamination is occurring.
Aerosol dust	This test influences the quality level of pixels contaminated by Saharan dusts. It is directly related to the SDI.
Distance to cloud	Pixels in the immediate vicinity of clouds are likely to be partly covered by cloud or affected by transparent undetected clouds.
Sea ice	The purpose of this test is to degrade the quality of pixels suspected to contain ice.
Satellite zenith angle	The test takes into account the fact that high satellite zenith angle is likely to lead to higher uncertainty because of higher atmospheric optical depth. The resulting indicator is directly linked to the satellite zenith angle.
SST correction	This test is based on the assumption that high SST corrections are associated with high uncertainties. It is directly linked to the value of the SST correction. It is only applied in the algorithm correction method.

Quality levels are designed to help users to filter out data that are not sufficiently good for their applications. It is essential to adopt the recommendation of the GHRSST formalised through the GDS v2 document. For infrared derived SST six quality levels are defined. 0: unprocessed; 1: cloudy, 2: bad, 3: suspect, 4 acceptable, 5 excellent.

The value of the quality level is determined by examining the values of three indicators: the SST mask indicator (resulting from several sub-indicators as explained above), the algorithm indicator and the SST correction indicator (only in the case of the algorithm correction method, see section 4.3). The poorest indicator will drive the value of the quality level.

Indicators enable to finely attribute quality levels to each pixel based on several considerations, however they are largely empirical and their tuning is manual and based on past experience.

3 Saharan Dust Index

Saharan dusts in the atmosphere have the effect of attenuating the signal received by the sensor therefore leading to an underestimation of SST. The SDI is a quantity calculated every hours for each cloud-free pixel. Its value is used to compute an empirical correction to SST retrievals affected by these aerosols and enters in the determination of the quality level.

Within the MSG/SEVIRI disk of view, Saharan dusts are mostly present in the Northern Tropical Atlantic region, in the Mediterranean Sea, in the Red Sea and in the Western part of the Arabic Sea. SDI is therefore computed for sea and lake pixels between 30°S and 50°N.

3.1 Night-time retrieval

3.1.1 Principle

The night-time SDI is defined by Merchant et al. (2006). It is computed as a linear combination of four SEVIRI channels:

$$\mathrm{SDI}_{\mathrm{night}} = S_1(T_{3.9} - T_{8.7}) + S_2(T_{10.8} - T_{12.0}) + S_3 \quad (2)$$

where the coefficients S_i are determined by regression using a database of simulated BTs performed using various concentrations of dust aerosol. Table 3 gives the values of each coefficient for both MSG1 and MSG2.

Table 3: Values of the coefficients for night-time SDI equation

	MSG1	MSG2
S_1	0.51	0.54
S_2	-0.86	-0.84
S_3	1.83	1.80

3.1.2 BT correction

SEVIRI instrument on-board MSG satellites is subject to contamination by the formation of a thin layer of ice on the optic of the instrument. Such contamination is affecting the 3.9 μm which is used for SDI computation. This problem is visible on the comparison between MSG3/SEVIRI and Metop-A/IASI presented by figure 1. One can observe a gradual contamination (for example between December and July 2013), and a brutal decontamination in July.

In order to avoid contamination/decontamination phenomenon to affect the computation of SDI, we apply a simple correction to the differences $(T_{3.9} - T_{8.7})$ and $(T_{10.8} - T_{12.0})$ prior to their usage: at midnight the correction term is the median of the difference between simulations and observations of BTS for all clear sky pixels in the domain 45°S and 45°N. at any other time, the correction is the interpolated 0h before and after.

The night SDI equation becomes:

$$\mathrm{SDI}_{\mathrm{night}} = S_1(T_{3.9} - T_{8.7} + \Gamma_1) + S_2(T_{10.8s} - T_{12.0s} + \Gamma_2) + S_3 \quad (3)$$

where Γ_1 and Γ_2 are the correction terms, $T_{10.8s}$ and $T_{12.0s}$ are smoothed BTs using a mean filter over 9×9 boxes in order to reduce noise in SDI fields (the same principle is classically used for SST computation).

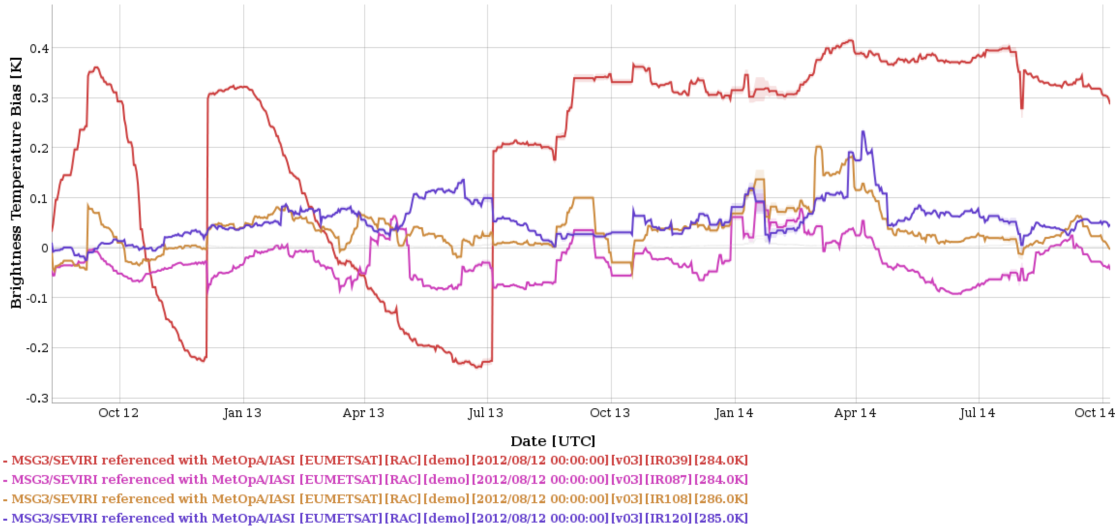

Figure 1: Illustration of the decontamination/drifting of the BT 3.9 μm *for Meteosat 10. Extracted from the Global Space-based Inter-Calibration System (http://gsics.wmo.int/)*

3.2 Day-time retrieval

Direct day-time estimation of SDI is not possible because the 3.9 m channel is contaminated by visible solar radiation. Instead, the following equation is used:

$$\mathrm{SDI}_{\mathrm{day}} = DS_1 T_{8.7} + DS_2 T_{10.8} + DS_3 T_{12.0} DS_4 T_{13.4} + DS_5 \tag{4}$$

where DS_i coefficients are determined by regression and interpolation. The regression is performed with night-time SDI and corresponding BTs at 8.7, 10.8, 12.0 and 13.4 μm in a [-12h, +12h] interval. It is performed regionally (for boxes of 251 $\times$ 251 pixels) and every hours using only clear sky pixels. An interpolation enable then to attribute DS_i coefficients to each pixel at any given time during the day and therefore to compute the daytime SDI.

4 SST algorithm

In this section we present the "classical" SST algorithm used in the control of the mask, and the algorithm correction method based on simulation of BTs. This section also present the BT simulations and the BT adjustment.

4.1 Non-linear SST algorithm

A classical non-linear SST algorithm is used to provide a first estimate of the SST. This estimate is used in various steps of the processing, it is referred to as the "classical" SST in the following:

- it is used in the calculation of an initial value of some indicators and QL (see section 2.3).
- it is used in the brightness temperature adjustment step (see section 4.2)
- it is the basis of the algorithm correction method (see section 4.3)

The non-linear SST algorithm is of the following form:

$$\mathrm{SST} = (a + b\, S_\Theta)\, T_{10.8} + (c + d\, S_\Theta + e\, T_{clim})(T_{10.8} - T_{12.0}) + f + g\, S_\Theta \quad (5)$$

where, $S_\Theta = sec(\Theta) - 1$ and Θ is the satellite zenith angle. T_{clim} is the climatological temperature. In practice, day-time and night-time algorithms differ slightly. The coefficient a, b, c, d and e are given in table 4.

Table 4: Values of the coefficients SST algorithm

		a	b	c	d	e	f	g
MSG1	day	0.98826	0.013554	0.0	0.853998	0.072930	1.410677	0.345426
	night	0.98826	0.013554	0.0	0.853998	0.072930	1.470028	0.382696
MSG2	day	0.98766	0.00417	0.39558	0.54305	0.05624	1.09287	0.94413
	night	0.98766	0.00417	0.39558	0.54305	0.05624	1.12698	0.97150

The difference $(T_{10.8} - T_{12.0})$ is highly sensitive to the atmosphere water vapour content. Since water vapour is the principal atmospheric component absorbing significantly infrared radiation at the wavelength used for SST retrieval, the term $(T_{10.8} - T_{12.0})$ is used in "split-window" algorithms to correct for absorption by water vapour in the atmosphere. However, this term is also particularly sensitive to radiometric noise; it is therefore smoothed over boxes of 11x31 pixels (scale at which the atmosphere is assumed to be homogeneous) by a mean filter, applied to clear/no ice pixels. This classical procedure reduces the noise in the retrieved SST.

Day-time and night-time algorithms are used for pixels with Sun Zenith Angle (SZA) below 90° and above 110° respectively. For pixels in twilight conditions ($90° < \mathrm{SZA} < 110°$), a linear combination of the two algorithms is used. For a given location (pixel) this combination depends on the value of the sun zenith angle and the limit angles of 90° and 110°:

$$\mathrm{SST} = k\, \mathrm{SST_{day}} + (1-k)\, \mathrm{SST_{night}} \text{ with } k = \frac{110 - \mathrm{SZA}}{110 - 90} \quad (6)$$

where $\mathrm{SST_{day}}$ and $\mathrm{SST_{night}}$ are the SSTs determined by the day-time and night-time algorithm respectively. The factor k is set to 0 and 1 when negative and above 1 respectively.

Since the coefficient of the SST algorithm are established using simulations from RTTOV radiative transfer model and de-biased against in-situ measurements, the retrieved SST is considered to be the sub-skin SST. One could apply a −0.17°C (Donlon et al., 2002) to get the skin SST. However this offset is only a very rough conversion term valid at large scale for wind speed exceeding 6 m/s^{-1}.

4.2 Brightness temperature simulation and adjustment

4.2.1 Brightness temperature simulation

Simulation of BTs are performed for each clear-sky sea or lake pixel using RTTOV v11. Input variable to RTTOV are described in section 2.2 and summarized here:

- A first guess of SST (SST^{guess}) provided by OSTIA dataset.
- Atmospheric temperature and humidity profiles from ECMWF ERA-interim dataset.
- MSG/SEVIRI filter function.

Simulations are performed at the time step of the input model data which is 3-hourly and for the four channels of interest for SST and SDI computation (3.9, 8.7, 10.8 and 12.0 μm).

4.2.2 Brightness temperature simulation adjustment

Before their usage in the algorithm correction or in the optimal estimation, BTs must be adjusted to correct for systematic differences with respect the observations. These differences can be due to:

- ECMWF water vapour profiles uncertainties
- Profile sampling
- RTTOV uncertainties
- MSG/SEVIRI filter function and calibration uncertainties

In a synthetic way, we use the difference between simulations and satellite observations (spatially and temporally smoothed) and interpret the differences as a correction. The description of the BT adjustment method is provided in detailed in Tomažić et al. (2014) for Metop/AVHRR.

The adjustment method used for MSG/SEVIRI SST data record is following the same general ideas which are adapted and presented hereafter.

The major hypothesis of the BT adjustment is that there is no average bias between the guess SST (used in BTs simulation) and the true SST. It is therefore crucial to properly filter out cases (pixels) where the simulated SST cannot be compared with guess SST (for example if there is a diurnal cycle or cloud contamination). This is done through several steps of filtering:

- Quality level filtering: only good quality SST retrievals are used (QL $\geq$ 4)
- Atmospheric dust aerosol filtering based on the dust aerosol indicator
- SST filtering: we ensure that “classical SST” and guess SST are close to each other (less than 1K difference)
- Elimination of cases where there is a risk of diurnal warming. Filter based on wind speed at 10 meters, solar zenith angle (Θ_{sol}) and a threshold on the difference between observed and simulated BTs.

- Only night-time pixels are kept except at high latitude where day-time pixels are allowed if the difference between simulated and observed BT at 10.8 μm is smaller than 0.5°C.

Filtered data are averaged temporally and spatially every day at 00h UTC using only slots at 00h UTC ± 3h on a 3-dimensional low resolution grid ($1 \times 1°$). An example of such field is shown on figure 2 (left). When computing the BT adjustment, these fields are averaged over 3 days (3 fields) and the result is smoothed out by applying a Gaussian kernel (radius = 5°, $\sigma = 2$). In order to fill in any remaining gaps, successive smoothing are applied with increasing kernel size. An example of adjustment field is shown on figure 2 (right).

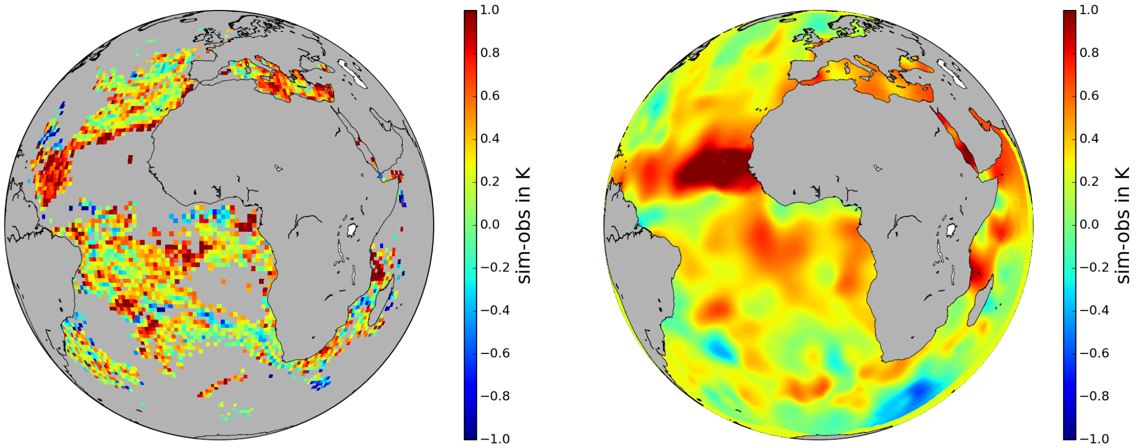

Figure 2: Left: Example of filtered data selected for BT adjustment for one day (at 00h UTC ± 3h) temporally and spatially averaged on a $1 \times 1°$ grid. Right: Example of BT adjustment field onto a 0.05° resolution regular grid.

The fields are then interpolated onto a 0.05° resolution regular grid (corresponding to the OSTIA grid) by bilinear interpolation. One such field is produced for each channels and at 00h UTC every day.

Figure 3 shows an example of the temporal evolution of the difference between simulations and observations before and after adjustment. During night-time, the adjustment brings the difference from approximately -0.3K to near zero on average. Whereas during day-time, this difference is brought to around 0.2K. This is explained by the diurnal variation of the surface temperature, the adjustment being computed using only night-time data.

BT simulations are computed with a 3-hourly time step, corresponding to NWP simulation time step. Adjustments are daily fields computed at 00h UTC, linearly interpolated to match the simulation time frame. Adjustments are added to BT simulations to produced adjusted BT simulations (3-hourly).

4.3 Algorithm correction

The method of algorithm correction was developed by Le Borgne et al. (2011), it is used in the operational processing of OSI SAF SST products from Metop-B and MSG/SEVIRI.

A so-called "simulated" SST (SST^{sim}) is computed from simulated BTs adjusted (see section 4.2) using the non-linear algorithms described in section 4.1.

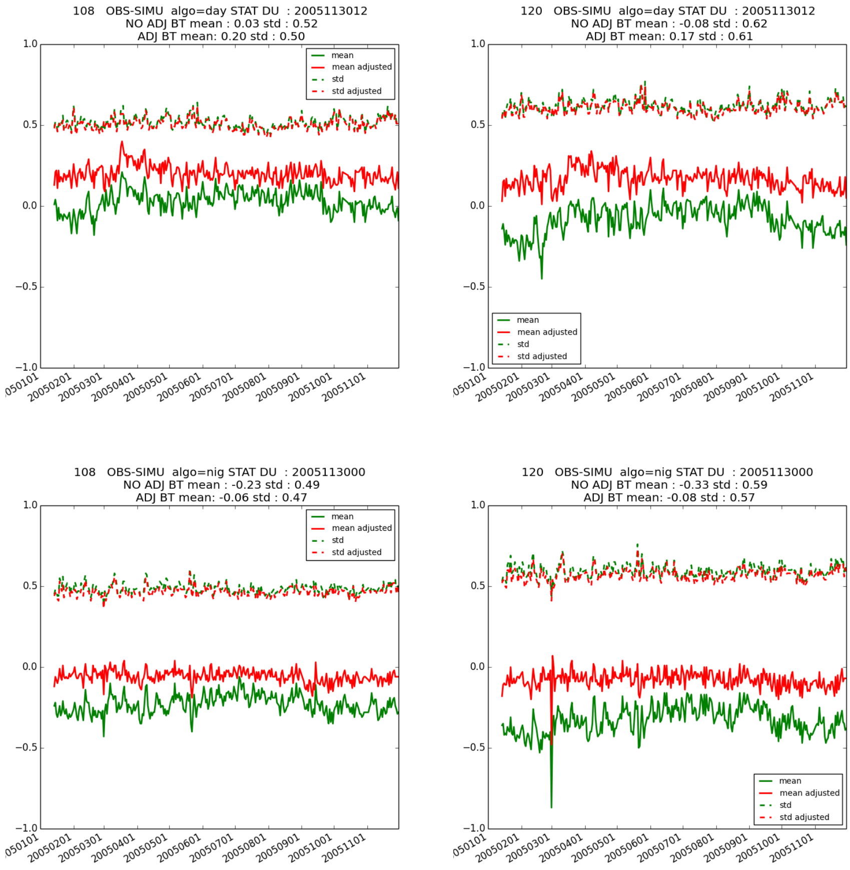

Figure 3: Control of the BT adjustment for channel 10.8 (left) and 12.0 (right) µm. Temporal evolution (2005) of the difference, in K, between simulated and observed BT in green; and between adjusted simulated and observed BT in red (global mean and standard deviation). Top: daytime; Bottom: night-time

Since the BT simulations have been adjusted to correct for uncertainties linked with RTTOV and atmospheric water vapour profiles, the only thing explaining the differences ($\Delta SST = SST^{sim} - SST^{guess}$) between the guess SST and the “simulated” SST, are attributed to intrinsic uncertainties originating from the SST algorithm itself.

In practice two SST algorithm correction fields are computed at the same time step as the simulations (3-hourly) corresponding to the two algorithms described in 4.1 (day and night). An example of algorithm correction fields is given on figure 4.

The 3-hourly day and night-time fields of algorithm correction are then linearly interpolated to the time of each slots. And the correction field to be applied to a particular slot is obtained by a weighed average of day and night-time fields using the factor k defined in equation 6 based on the sun zenith angle.

The corrected SST is computed by subtracting the algorithm correction to the “classical” SST.

4.4 SDI correction

The SST retrieval method described above does not handle cases where dust aerosols are present in the atmosphere. It is therefore important to consider these cases. It has been shown that

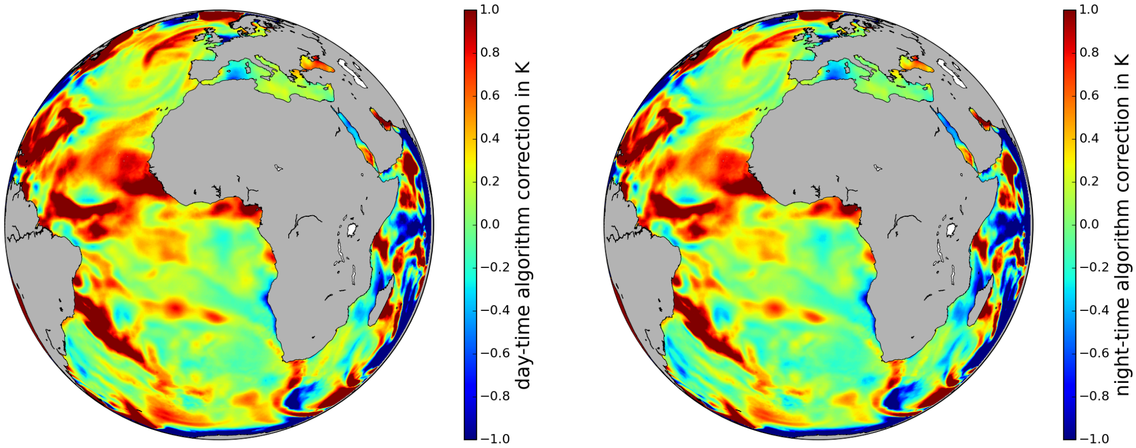

Figure 4: Algorithm correction fields for day-time (left) and night-time (right) algorithms.

the SDI (see section 3) can be used to correct the retrieved SST in some cases (Merchant et al. (2006)).

The SDI correction is based on the definition of a quadratic function of the SDI (φ(SDI)) that models the average error in SST retrievals due to the presence of Saharan dusts. This function is applied on a pixel basis.

$$\varphi(\mathrm{SDI}) = a_0 + a_1\mathrm{SDI} + a_2\mathrm{SDI}^2 \tag{7}$$

The coefficients are determined by regression using the a sub sample of the Matchup Dataset (MDS). In order to avoid correcting SSTs where the SDI is not significant, we ensure that below a limit value of SDI, the correction is null. We consider that for SDI below 0, the retrieval of SST is not impacted by Saharan dusts, and therefore no correction is applied. For high values of SDI (above 0.4) we consider that the correction is not reliable, therefore no correction is applied in these cases and the quality level is set to 2 (bad).

5 Hourly synthesis and final product

SST retrieval is done for each 15 minutes slot the concatenation into hourly L3C products is done as a post processing. The method used to create these hourly synthesis is described here.

For the hourly product at H (H being a round hour) the contributing slots are H-30, H-15, H and H+15 minutes. No averaging or interpolation is done. The SST for a given pixel is directly extracted from one of the slot contributing to the hourly synthesis. For each pixel, there are potentially 4 candidates (corresponding to the 4 contributing slots). The primary criteria of choice is the quality level: only the best QL is selected. If several candidate have a QL equal to the best QL then the pixel closer in time to H is selected.

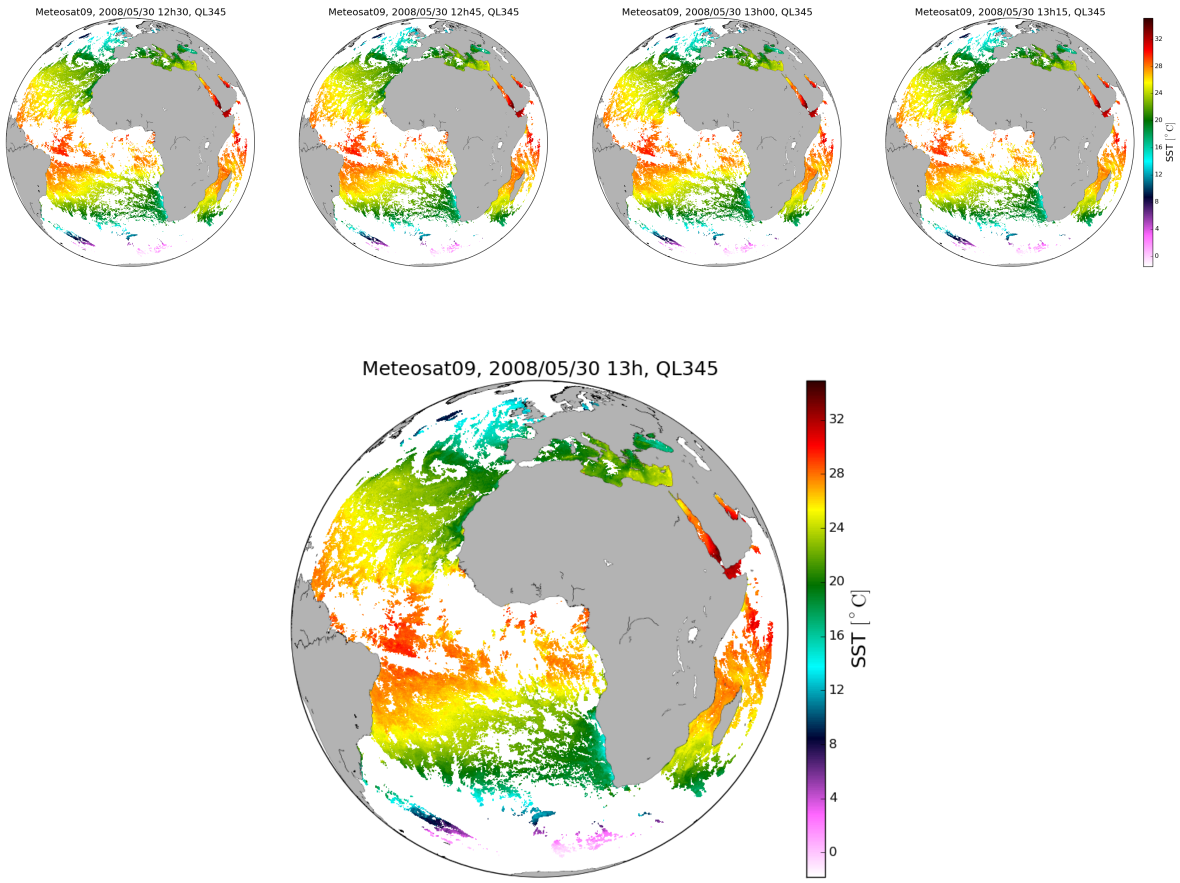

Figure 5: Example of hourly synthesis of SST. Top row: four slots of SST; bottom map: hourly L3C SST

The final dataset is obtained by re-mapping hourly SST onto a 0.5° regular grid by using a nearest neighbour approach.

6 Single Sensor Error Statistics

SSES are required by the GHRSST Data Specification (GDS) v2. They consist in bias and standard deviation of the error between SST retrieval and drifting buoys measurements. They shall be provided per pixel.

For MSG/SEVIRI SST data record bias and standard deviation of the difference between satellite retrieval and drifting buoys are computed per satellite, per QL and for day and night-time using the whole MDS. Bias and standard deviation are then attributed to each pixel according to its QL.

Values of the SSES bias and standard deviation can be found in the [RD.2] in table 4 of the section "Overall statistics“.

References

Atkinson, C., Rayner, N., Kennedy, J., and Good, S. (2014). An integrated database of ocean temperature and salinity observations. *Journal of Geophysical Research-Ocean*, 119:7139–7163.

Dee, D. and 35 co-authors (2011). The era-interim reanalysis: Configuration and performance of the data assimilation system. *Quarterly Journal of Royal Meteorology Society*, 137:553–597.

Donlon, C. J., Martin, M., Stark, J., Roberts-Jones, J., Fiedler, E., and Wimmer, W. (2012). The operational sea surface temperature and sea ice analysis (OSTIA) system. *Remote Sensing of Environment*, 116:140—-158.

Donlon, C. J., Minnett, P. J., Gentemann, C., Nightingale, T. J., Barton, I. J., Ward, B., and Murray, M. J. (2002). Toward improved and validation of satellite and sea surface and skin temperature and measurements and for climate and research. *Journal of Climate*, 15:353–359.

Le Borgne, P., Roquet, H., and Merchant, C. (2011). Estimation of sea surface temperature from the spinning enhanced visible and infrared imager, improved using numerical weather prediction. *Remote Sensing of Environment*, 115(1):55–65.

McCain, E. P., Pichel, W. G., and Walton, C. C. (1985). Comparative performance of AVHRR-based multichannel sea surface temperature. *Journal of Geophysical Research*, 90:11587–11601.

Merchant, C. J., Embury, O., Le Borgne, P., and Bellec, B. (2006). Saharan dust in nighttime thermal imagery: Detection and reduction of related biases in retrieved sea surface temperature. *Remote Sensing of Environment*, 104(1):15–30.

Merchant, C. J., Filipiak, M. J., Le Borgne, P., Roquet, H., Autret, E., Piollé, J.-F., and Lavender, S. (2008). Diurnal warm-layer events in the western mediterranean and European shelf seas. *Geophys. Res. Lett.*, 35(4):1–4.

Roberts-Jones, J., Fiedler, E., and Martin, M. (2012). Daily, global, high-resolution sst and sea ice reanalysis for 1985-2007 using the ostia system. *Journal of Climate*, 25(18):6215–6232.

Saunders, R., Matricardi, M., and Brunel, P. (1999). An improved fast radiative transfer model for assimilation of satellite radiance observations. *Quarterly Journal of the Royal Meteorological Society*, 125:1407–1425.

Tomažić, I., Le Borgne, P., and Roquet, H. (2014). Assessing the impact of brightness temperature simulation adjustment conditions in correcting Metop-A SST over the mediterranean sea. *Remote Sensing of Environment*, 146:214–233.